A study on rupture process and multiple fault segments in 2004 Indian Ocean Tsunami

Pawin Situngnoen and Chaiwoot Boonyasiriwat

ABSTRACT

The occurrence of the 2004 Indian Ocean Tsunami had two phenomena, the rupture process and the multiple fault segments of tsunami source characteristics. There are several tsunami source characteristics used in tsunami simulation, but this work focuses on 5 and 6 fault segments of tsunami source. To study the effect of among of fault segments and determine the best tsunami source characteristics at the Bay of Bengal, the 2D linearized shallow-water equations are solved by using the explicit finite difference method. The tsunami gauge data at some stations are used to compare the accuracy of tsunami simulated results. From my results, we find that the tsunami profile of 6 fault segments mostly fits the tsunami gauge data in both cases of dynamic rupture and static rupture. However, the satellite altimeter data must be used to compare the accuracy of tsunami simulated results, too. We have some issue about the reading process on our satellite altimeter data. This problem is going solved and the satellite altimeter data is going studied in future work.

REVIEW OF RUPTURE PROCESS

The rupture process of the 2004 Indian Ocean Tsunami Event was studied (Bilham, 2005; Ammon and et al., 2005; Lay and et al., 2005). After we review their works, we find that the important parameters of the rupture process are a total duration time, a rise time, and a rupture velocity when an underwater earthquake uplifts.

In addition, we know that the rupture zone of this tsunami covers northward from the epicenter (3.316^{o}N and 95.854^{o}E) along about 1,300 km (Ammon and et al., 2005). The rupture zone can be separated into a region of main tsunami excitation and region of weak tsunami excitation. However, Lay and et al. (2005) subdivided the rupture zone into three segments; Sumatra, Nicobar and Andaman Segments that can be presented in Figure 1.

From the study of Lay and et al. (2005), the region of main tsunami excitation covers the Sumatra and Nicobar Segments along 745 km, while the region of weak tsunami excitation covers only the Andaman Segment. In addition, each fault segments had their seismic parameters that are presented in Figure 2.

Moreover, the seafloor uplifted by two phenomena. First one is called "rapid slip" by using the total duration time about 10 minutes with the rupture velocity 2.5 km/sec (Lay and et al., 2005; Bilham, 2005). The another one is called "slow slip" by using the total duration time about 1 hour with the rupture velocity 0.75 km/sec (Lay and et al., 2005).

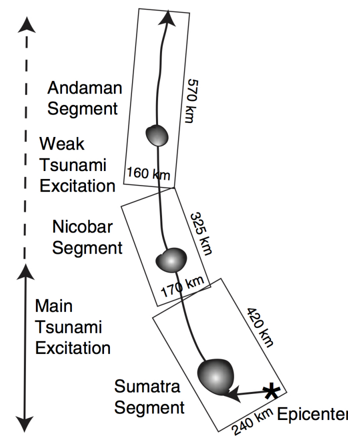

Figure 1: Three segments of rupture zone; Sumatra, Nicobar and Andaman Segments (Lay and et al., 2005).

Segment	Length (km)	Width (km)	Rake (deg)	Dip (deg)	Slip (m)	Rise time (min)
Sumatra	420	240	110	14	5-10	1 (rapid slip)
Nicobar	325	170	120	15	5	4-6 (rapid slip)
Andaman	570	160	150	18	<2	58 (slow slip)

Figure 2: Some of the seismic parameters and the rise time of underwater earthquake's uplift for three fault segments.

In all of the previous studies, they concluded that the rapid slip occurred in the region of main tsunami excitation when underwater earthquake uplifts. In addition, the slow slip occurred in the region of weak tsunami excitation.

In addition, the rupture process of this event is related to multiple fault segments of an underwater earthquake that is reviewed in the next section.

REVIEW OF MULTIPLE FAULT SEGMENTS

The 2004 Indian Ocean Tsunami was generated not only by the rupture process when the underwater earthquake uplifts, but also by multiple fault segments. The multiple fault segments are used as multiple tsunami sources that are called tsunami source characteristics.

The tsunami source characteristics necessarily require a set of seismic parameters that are consists of a center of fault (x_0, y_0), focal depth (d), length of fault (L), width of fault (W), slip displacement (Δ), strike angle (ϕ), dip angle (δ), and rake angle (λ). Figure 3 presents the various tsunami source characteristics for simulation (Koh and et al., 2009; Guo and et al., 2015; Kowalik and et al., 2005; Son and et al., 2011; Arcas and Titov, 2006; Grilli and et al., 2007; Rhie and et al., 2007; Lay and et al., 2005).

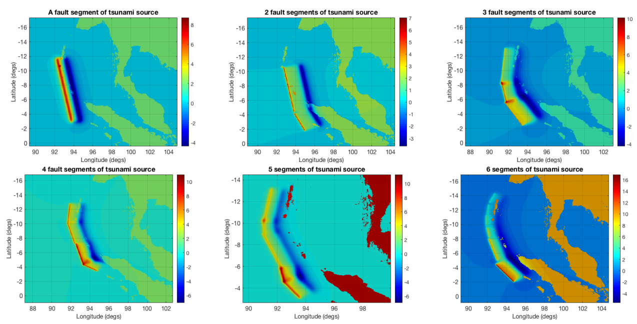

Figure 3: 6 types of tsunami source characteristics used in the simulation of the 2004 Indian Ocean Tsunami.

Grilli and et al. (2007) and Ioualalen and et al. (2007) studied the constraints of tsunami source and effect of dispersion by using the 5 fault segments of tsunami source characteristics.

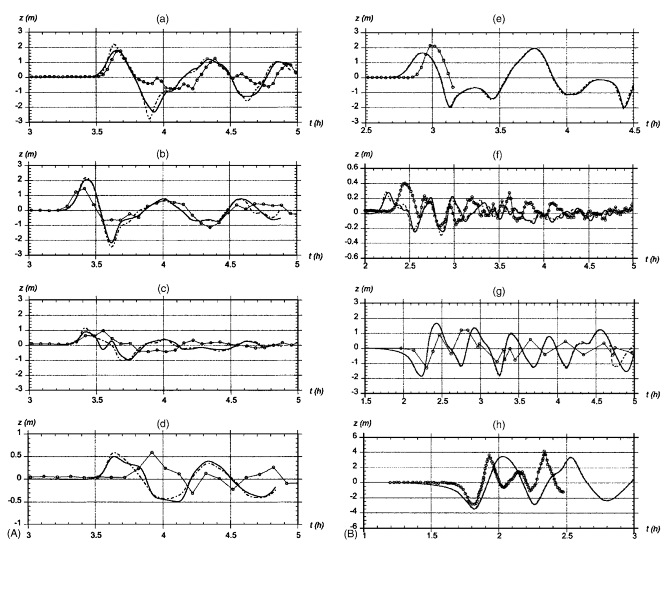

Figure 4: Tsunami profile and simulated result at some selected gauge stations (a) Hannimaadhoo; (b) Male; (c) Gan; (d) Diego Garcia; (e) Columbo; (f) Cocos Island; (g) Taphao-Noi; and (h) Mercator yacht (Grilli and et al., 2007).

They simulated the tsunami propagation using FUNWAVE and GEOWAVE programs. These programs solve the Boussinesq and shallow-water equations by a higher-order finite volume method. They predicted the tsunami profile at some gauge stations and satellite JASON-1's track. Figure 4 and 5 present their simulated results by comparing with the tsunami gauge data and altimeter data, respectively.

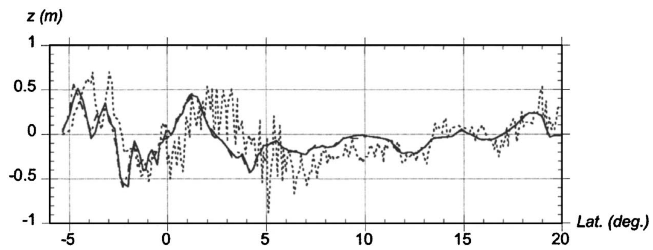

Figure 5: The numerical result and the satellite's altimeter data during record the sea surface elevation at the Indian Ocean in this event (Grilli and et al., 2007).

The 6 fault segments of tsunami source characteristic for the 2004 Indian Ocean Tsunami is used in the study of Lay and et al. (2005) and Rhie and et al. (2007). However, this work focuses only on the work of Rhie and et al. (2007).

The tsunami source characteristic of 6 fault segments in Rhie and et al. (2007) is used to study the best seismic model in tsunami simulation by Poisson and et al. (2011). In the work of Poisson and et al. (2011), they simulated the tsunami propagation with the altimeter data that is presented in Figure 6.

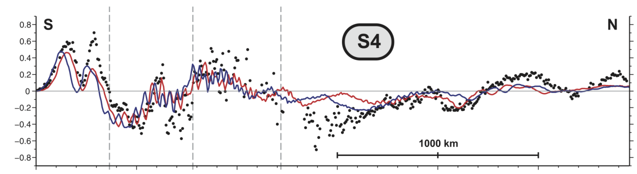

Figure 6: The numerical result and the satellite's altimeter data (Poisson and et al., 2011).

All of the previous studies motivate this work to study about the 5 and 6 fault segments of tsunami source characteristics in tsunami simulation. Moreover, our simulated results are compared with tidal gauge data and satellite altimeter data.

EXPERIMENT OF MULTIPLE FAULTS

The Governing Equations

The 5 and 6 fault segments of tsunami source are used in this work. The effect of fault number is tested by using the 2D linearized shallow-water equations with the PML boundary condition as

$$\frac{\partial \eta}{\partial t} = -(\sigma_x+\sigma_y)\eta - \sigma_x\sigma_y\psi - H\left(\frac{\partial u}{\partial x}+\frac{\partial v}{\partial y}\right), \quad (1)$$

$$\frac{\partial u}{\partial t} = -\sigma_x u - \bar{U}\frac{\partial u}{\partial x} - \bar{V}\frac{\partial u}{\partial y} - g\frac{\partial \eta}{\partial x}, \quad (2)$$

$$\frac{\partial v}{\partial t} = -\sigma_x v - \bar{U}\frac{\partial v}{\partial x} - \bar{V}\frac{\partial v}{\partial y} - g\frac{\partial \eta}{\partial y}, \quad (3)$$

$$\frac{\partial \psi}{\partial t} = \eta, \quad (4)$$

where η is a sea-surface elevation, (u, v) are horizontal velocities, H is a total water column by $H = \eta + d$ (d is unperturbed water depth), $(\bar{U}, \bar{V})$ are the averaged velocities (that equal to 1 in this work), (σ_x, σ_y) are the absorption coefficients, and ψ is an auxiliary field.

For solving the governing equations, the staggered grid of finite difference and the first-order upwind are used for solving of the conservation of momentum and mass equations, respectively.

The numerical index form of the governing equations can be written as

$$\begin{aligned}
\psi^{n+1}_{i,j} &= \psi^n_{i,j} + (\Delta t)\eta^n_{i,j},\\
u^{n+1}_{i,j} &= \left[1-(\Delta t)(\sigma_x)_{i,j}\right]u^n_{i,j} - g\frac{\Delta t}{\Delta x}\left(\eta^n_{i+1,j}-\eta^n_{i,j}\right)\\
&- \frac{1}{2}\frac{\Delta t}{\Delta x}\bar{U}\left(u^n_{i+1,j}-u^n_{i-1,j}\right) - \frac{1}{2}\frac{\Delta t}{\Delta y}\bar{V}\left(u^n_{i,j+1}-u^n_{i,j-1}\right),\\
v^{n+1}_{i,j} &= \left[1-(\Delta t)(\sigma_y)_{i,j}\right]v^n_{i,j} - g\frac{\Delta t}{\Delta y}\left(\eta^n_{i,j+1}-\eta^n_{i,j}\right)\\
&- \frac{1}{2}\frac{\Delta t}{\Delta x}\bar{U}\left(v^n_{i+1,j}-v^n_{i-1,j}\right) - \frac{1}{2}\frac{\Delta t}{\Delta y}\bar{V}\left(v^n_{i,j+1}-v^n_{i,j-1}\right),\\
\eta^{n+1}_{i,j} &= \left[1-(\Delta t)(\sigma_x+\sigma_y)_{i,j}\right]\eta^n_{i,j} - \Delta t(\sigma_x\sigma_y)_{i,j}\psi^n_{i,j}\\
&- \frac{\Delta t}{\Delta x}\left(u^+_e H^n_{i,j} + u^-_e H^n_{i+1,j} - u^+_w H^n_{i-1,j} - u^-_w H^n_{i,j}\right)\\
&- \frac{\Delta t}{\Delta y}\left(v^+_n H^n_{i,j} + v^-_n H^n_{i,j+1} - v^+_s H^n_{i,j-1} - v^-_s H^n_{i,j}\right),
\end{aligned}$$

where

$$\begin{aligned}
u^+_e &= 0.5\left(u^n_{i,j}+|u^n_{i,j}|\right), & u^-_e &= 0.5\left(u^n_{i,j}-|u^n_{i,j}|\right),\\
u^+_w &= 0.5\left(u^n_{i-1,j}+|u^n_{i-1,j}|\right), & u^-_w &= 0.5\left(u^n_{i-1,j}+|u^n_{i-1,j}|\right),\\
v^+_n &= 0.5\left(v^n_{i,j}+|v^n_{i,j}|\right), & v^-_n &= 0.5\left(v^n_{i,j}-|v^n_{i,j}|\right),\\
v^+_s &= 0.5\left(v^n_{i,j-1}+|v^n_{i,j-1}|\right), & v^-_s &= 0.5\left(v^n_{i,j-1}+|v^n_{i,j-1}|\right).
\end{aligned}$$

Physical Domain

The physical domain in this work is the Bay of Bengal region that is located at latitude 15^oS to 25^oN and longitude 70^oE to 105^oE (Figure 7). We use the topography and bathymetry data from 2-minute guided global relief data (ETOPO2) [http:www.ngdc.noaa.gov/mgg/fliers/01mgg04.html] that contain the $1,050 \times 1,200$ grid points with $3,712$ meters of a grid spacing.

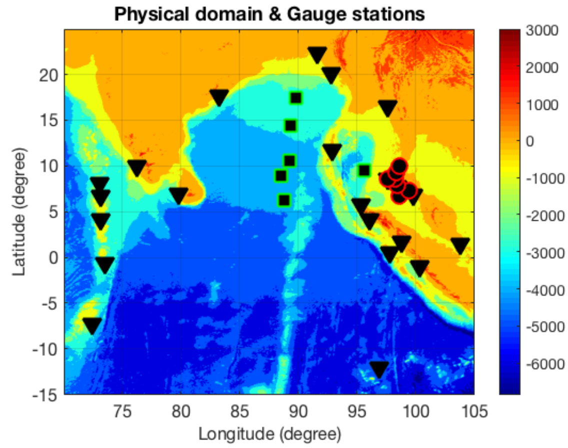

Figure 7: The Bay of Bengal region and our gauge stations.

NUMERICAL RESULTS

After we simulate the propagation of 2004 Indian Ocean Tsunami, we record tsunami profile at our gauge stations. However, we select some of the gauge stations to compare the simulated results with tsunami gauge data. Now we have two cases of simulated results that are the case of dynamic rupture (underwater earthquake uplifts at a different time) and the case of static rupture.

Case of Dynamic Rupture

Tsunami profile at some selected gauge stations are presented as

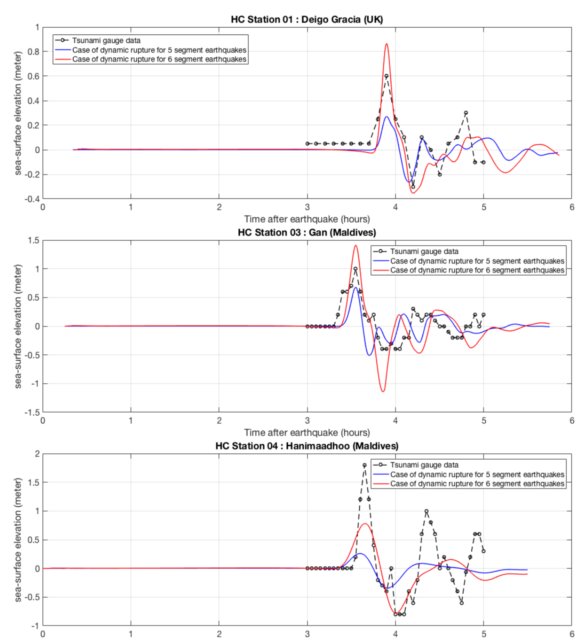

From these result, we can notice that tsunami profile of 6 fault segments can fit tsunami gauge data more than 5 fault segments.

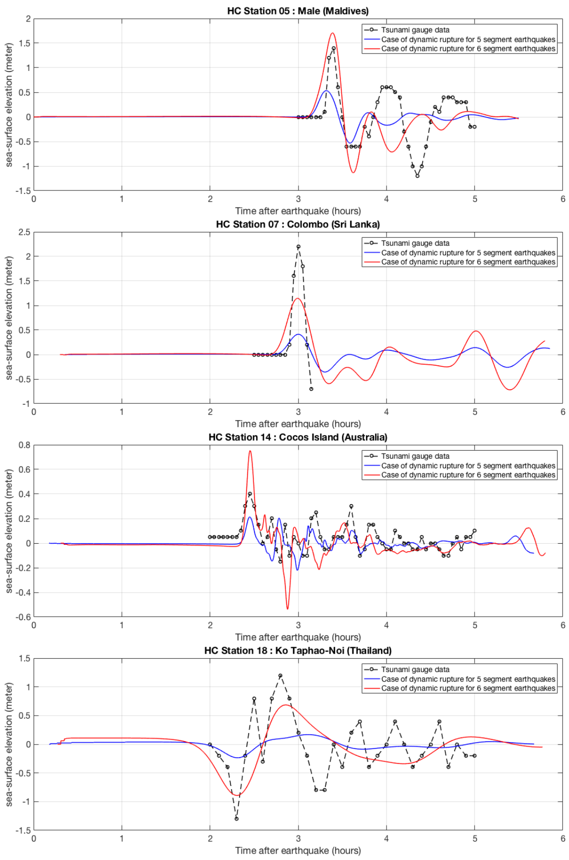

Case of Static Rupture

Tsunami profile at some selected gauge stations are presented as

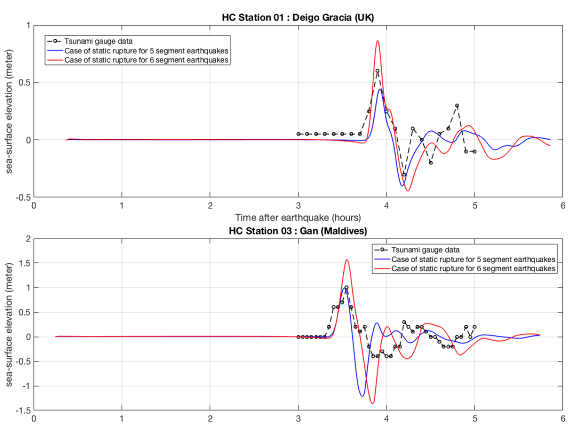

From these result, we can notice that tsunami profile of 6 fault segments can fit tsunami gauge data more than 5 fault segments like in case of dynamic rupture. Thus, we can suppose that amount of fault segments can affect the accuracy of tsunami predictions.

However, we have another type of tsunami data that is the satellite altimeter data. Therefore, the detail about the preparation of satellite data is present in the next section.

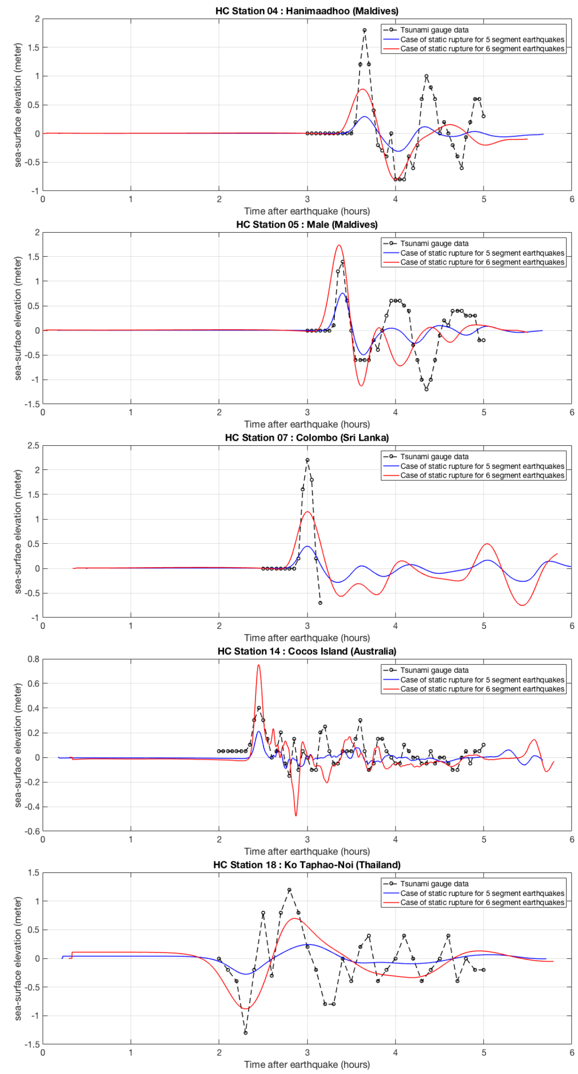

SATELLITE ALTIMETER DATA

In the 2004 Indian Ocean Tsunami, the satellite altimeter (JASON-1) can first observe tsunami wave in the Indian Ocean by detecting sea surface height. The sea surface height data are published as the following link https://opendap.jpl.nasa.gov/.

After we finish the process of file reading, the satellite altimeter data is presented in Figure 8. In addition, Figure 9 and 10 are presented the satellite altimeter data of the previous works.

Notice that our satellite altimeter data is incorrect. This means that we have some problem with a technique for the process of file reading. Thus, this part of our work is continuously done.

SUMMARY

For the 2004 Indian Ocean Tsunami, the rupture process of multiple fault segments is studied by several re-

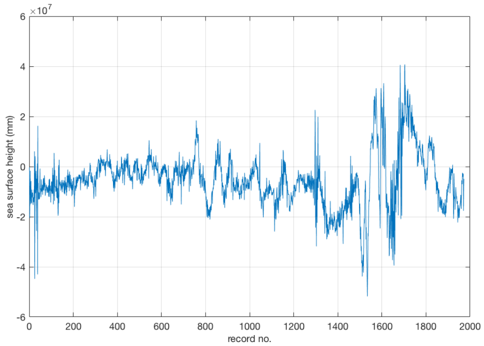

Figure 8: The satellite altimeter data in this work.

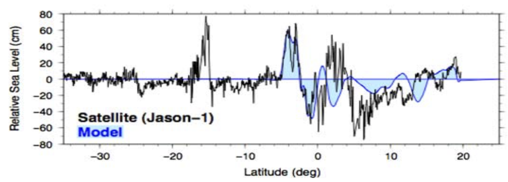

Figure 9: The satellite altimeter data of Arcas and Titov (2006).

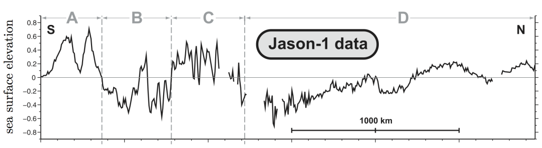

Figure 10: The satellite altimeter data of Poisson and et al. (2011).

searchers. They concluded that this tsunami has two rupture process; rapid slip and slow slip.

Furthermore, the several tsunami researchers proposed the various tsunami source characteristics. Thus, this work would like to study two type of tsunami source characteristics that are 5 and 6 fault segments of tsunami source.

The 2D linearized shallow-water equations with PML are solved by using The staggered-grid and first-order upwind schemes of explicit finite difference method. The physical domain in this work is the Bay of Bengal region that is located at latitude 15^oS to 25^oN and longitude 70^oE to 105^oE.

After we simulate the propagation of 2004 Indian Ocean Tsunami, we record tsunami profile at some selected gauge stations with gauge data. In addition, we have two cases of simulated results that are the case of dynamic rupture and the case of static rupture. We found that tsunami profile of 6 fault segments can fit tsunami gauge data more than 5 fault segments in two cases. Thus, we can suppose that amount of fault segments can affect the accuracy of tsunami predictions.

Furthermore, the satellite altimeter data is used in this work. However, we have some issue about file reading that results in the incorrect satellite altimeter data. Thus, this problem is continuously solved in future work.

REFERENCES

Ammon and et al., 2005, Rupture process of the 2004 sumatra-andaman earthquake: Science, **308**, 1133–1139.

Arcas and Titov, 2006, Sumatra tsunami: lessons from modeling: Surveys Geophysics, **27**, 679–705.

Bilham, 2005, A flying start, then a slow slip: Science, **308**, 1126–1127.

Grilli and et al., 2007, Source constraints and model simulation of the december 26, 2004, indian ocean tsunami: Journal of Waterway, Port, Coastal, and Ocean Engineering, **133**, 414–428.

Guo and et al., 2015, Time?space decoupled explicit method for fast numerical simulation of tsunami propagation: Pure Applied Geophysics, **172**, 569–587.

Ioualalen and et al., 2007, Modelling of the 26 december 2004 indian ocean tsunami: Case study of impact in thailand: Journal of Geophysics Research, **112**.

Koh and et al., 2009, Simulation of andaman 2004 tsunami for assessing impact on malaysia: Journal of Asian Earth Sciences, **36**, 74–83.

Kowalik and et al., 2005, Numerical modeling of the global tsunami: Indonesian tsunami of 26 december 2004: Science of Tsunami Hazards, **23**, 40–56.

Lay and et al., 2005, The great sumatra-andaman earthquake of 26 december 2004: Science, **308**, 1127–1133.

Poisson and et al., 2011, Is there a best source model of the sumatra 2004 earthquake for simulating the consecutive tsunami?: Geophysical Journal International, **185**, 1365–1378.

Rhie and et al., 2007, Slip of the 2004 sumatra?andaman earthquake from joint inversion of long- period global seismic waveforms and gps static offsets: Bulletin of the Seismological Society of America, **97**.

Son and et al., 2011, Nested and multi-physics modeling of tsunami evolution from generation to inundation: Ocean Modelling, **38**, 96–113.